

## IMPLICIT THREE-DIMENSIONAL FINITE ELEMENT SOLUTIONS OF EULER EQUATIONS IN CONSERVATION VARIABLES

### Denis A.F. de Souza

Laboratory for Computational Methods in Engineering and Dept. of Civil Engineering, COPPE/Federal University of Rio de Janeiro  
PO Box 68552, Rio de Janeiro, RJ, 21949-900, Brazil  
[denis@lamce.ufrj.br](mailto:denis@lamce.ufrj.br)

### Paula A. Sesini

Center for Parallel Computations and Dept. of Civil Engineering, COPPE/Federal University of Rio de Janeiro (UFRJ)  
PO Box 68506, Rio de Janeiro, RJ, 21945-970, Brazil  
[psesini@coc.ufrj.br](mailto:psesini@coc.ufrj.br)

### Alvaro L.G.A. Coutinho

Center for Parallel Computations and Dept. of Civil Engineering, COPPE/Federal University of Rio de Janeiro (UFRJ)  
PO Box 68506, Rio de Janeiro, RJ, 21945-970, Brazil  
[alvaro@nacad.ufrj.br](mailto:alvaro@nacad.ufrj.br)

**Abstract.** An implicit implementation of the SUPG formulation with shock capturing for 3D inviscid compressible flows in conservation variables is presented. A shock capturing formulation, derived initially in entropy variables, was implemented plus a freezing technique to avoid residual stagnation and to improve convergence towards steady state. Local time-stepping and Jacobian-Free Newton-Krylov methods are also employed to improve convergence. Classical numerical examples of high speed flows governed by the Euler equations, such as, the one-dimensional normal shock and the two-dimensional oblique and reflected shocks are presented.

**Keywords.** High speed flows, Euler equations, Finite elements.

### 1. Introduction

The compressible Euler equations for high speed flows have been extensively studied in the 80s and 90s. One of the most used numerical methods is finite elements, which has strong mathematical background, good accuracy and handles naturally complex geometries. However, today's computing power is still insufficient to resolve all the physics involved in large-scale problems, even when seeking steady state solutions. The most widely technique used to solve steady compressible problems is to start from an initial guess and march in time until steady state is reached. In other words, drive steady state solutions with a pseudo-transient analysis. Within the finite element context, such calculations become possible after the papers by Tezduyar and Hughes (1982, 83) where stabilized methods were developed. Therefore, stabilized finite element methods are now used for simulations of viscous and inviscid compressible flows. Important steps in the application of the methods to compressible flows were the generalization to the system of Euler equations expressed in terms of entropy variables (Hughes *et al.*, 1986), the development of shock capturing terms, sometimes called artificial viscosity models based on the residual of the Euler equations as in Shakib (1988) and Almeida and Galeão (1996) after reformulation of the methods for entropy variables. On the theoretical side, the achievements included proofs of convergence of the methods for systems of conservation laws (Johnson *et al.*, 1990).

In the present paper, we use an implicit semi-discrete stabilized finite element method, based on a SUPG formulation plus a shock capturing operator derived from entropy variables, for space discretization of the Euler equations of compressible gas flow and compare two non-linear strategies: a fully implicit with exact Jacobian and other with an approximate Jacobian. The comparison is done in terms of computer time usage for problems in different flow regimes: subsonic and supersonic.

The alternative approach for solving non-linear PDEs used here is the so-called Jacobian Free Newton-Krylov (JFNK) methods, that follows Johan *et al.* (1991) and Knoll and Keyes (2004). Such methods reduce memory requirements and may accelerate non linear convergence. We compare computer processing times and memory savings for both cases.

Furthermore, two convergence acceleration techniques are employed. The freezing of the shock capturing operator, as in Catabriga and Coutinho (2002), that reduces significantly the residual norm in several orders of magnitude and the local time-stepping approach which decreases the residual norm as well. The main idea of this paper is to test the two acceleration techniques with the usual approach and the JFNK method, with structured and unstructured grids. We are especially interested in the convergence of high speed flows with shocks.

The paper is organized as follows. In Section 2, the governing equations for compressible inviscid flows are described. In Section 3, we present the stabilized finite element formulation and the convergence acceleration

techniques are briefly described in Section 4. Section 5 presents results of some numerical tests and some conclusions are drawn in Section 6.

## 2. Governing equations

The quasi-linear form of the three-dimensional Euler equations in conservation variables without source terms follows Hirsch (1992) and are an inviscid system of conservation laws represented by,

$$\mathbf{U}_{,t} + \mathbf{F}_{i,i} = 0 \quad \text{in } \Omega \times [0, T_{max}] \quad (1)$$

where for  $\Omega \subset \mathbb{R}^3$  and  $t \in [0, T_{max}]$ , the vector of conservative variables  $\mathbf{U}$ , and the vector of Euler fluxes  $\mathbf{F}_i$  are given respectively by:

$$\mathbf{U} = \begin{Bmatrix} U_1 \\ U_2 \\ U_3 \\ U_4 \\ U_5 \end{Bmatrix} = \rho \begin{Bmatrix} 1 \\ u_1 \\ u_2 \\ u_3 \\ e \end{Bmatrix} \quad (2)$$

$$\mathbf{F}_i = \rho u_i \begin{Bmatrix} 1 \\ u_1 \\ u_2 \\ u_3 \\ e \end{Bmatrix} + p \begin{Bmatrix} 0 \\ \delta_{1i} \\ \delta_{2i} \\ \delta_{3i} \\ u_i \end{Bmatrix} \quad (3)$$

In Equations (2) e (3),  $\rho$  is the density of the fluid,  $\mathbf{u} = [u_1, u_2, u_3]^T$  is the velocity vector and  $e$  is the total energy density, that is the sum of the internal energy  $E$  and the density of kinetic energy  $\|\mathbf{u}\|^2/2$ ,  $p$  is the thermodynamic pressure and  $\delta_{ij}$  is the Kronecker delta. Assuming that the fluid obeys the perfect gases law, the constitutive relations are given by the following expressions,

$$t = c_v T \quad (4)$$

$$p = (\gamma - 1) \rho t \quad (5)$$

where  $c_v$  is the specific heat at constant volume,  $T$  is the absolute temperature,  $\gamma = c_p/c_v$  and  $c_p$  is the specific heat at constant pressure. Alternatively, Eq. (1) may be written as

$$\mathbf{U}_{,t} + \mathbf{A}_x \mathbf{U}_{,x} + \mathbf{A}_y \mathbf{U}_{,y} + \mathbf{A}_z \mathbf{U}_{,z} = 0 \quad \text{in } \Omega \times [0, T_{max}] \quad (6)$$

where the Jacobian matrices  $\mathbf{A}_i$ , for  $i = x, y, z$  are defined as

$$\mathbf{A}_i = \frac{\partial \mathbf{F}_i}{\partial \mathbf{U}} \quad (7)$$

The Euler equations can be recast as a symmetric form through a change of variables from conservative to entropy variables ( $\mathbf{V}$ ) as derived in Hughes *et al.* (1986). We define a scalar function named generalized entropy function by

$$H(\mathbf{U}) = \rho s \quad (8)$$

where  $s = \ln(p/\rho\gamma) + s_0$ , is the physical entropy by unity mass and  $s_0$  a reference entropy. Thus, we may introduce the entropy variables  $\mathbf{V} = H_{,U}$  and the relationship  $\mathbf{U} \rightarrow \mathbf{V}$  is given by,

$$\mathbf{V} = \left\{ \begin{array}{l} V_1 \\ V_2 \\ V_3 \\ V_4 \\ V_5 \end{array} \right\} = \frac{1}{\rho t} \left\{ \begin{array}{l} -U_5 + \rho t(\gamma + 1 - s) \\ U_2 \\ U_3 \\ U_4 \\ -U_1 \end{array} \right\} \quad (9)$$

Therefore the Euler equations in entropy variables are alternatively written as

$$\tilde{\mathbf{A}}_0 \mathbf{V}_{,t} + \tilde{\mathbf{A}}_i \mathbf{V}_{,i} = 0 \quad \text{in } \Omega \times [0, T_{max}] \quad (10)$$

where  $\tilde{\mathbf{A}}_0 = \mathbf{U}_{,V}$  is symmetric positive definite and  $\tilde{\mathbf{A}}_i = \mathbf{A}_i \tilde{\mathbf{A}}_0$  is symmetric. The finite element formulation of the present work is based in the discretization of Eq. (10). We specify suitable boundary and initial conditions to it.

Assuming that the problem domain has a contour  $\Gamma = \Gamma_g \cup \Gamma_h$ , the Euler equations admit boundary conditions of two types:

- Dirichlet conditions:  $G(\mathbf{U}) = g(t)$  in  $\Gamma_g$  where  $G(\mathbf{U})$  is a nonlinear vector function of conservation variables,  $\mathbf{U}$  and  $g(t)$  are the prescribed values of  $G$  at the contour  $\Gamma_g$  of  $\Omega$ .
- Neumann conditions:  $\mathbf{F}_i$  is given at the contour  $\Gamma_h$  of  $\Omega$ . This condition is similar to specify values of first order derivatives of some or every dependent variables of the problem.

### 3. Finite element discretization

The semi-discrete formulation is characterized by a finite element discretization in space followed by a finite difference discretization in time. It is considered the space domain  $\Omega$  divided in  $nel$  elements,  $\Omega^e$ ,  $e = 1, 2, \dots, nel$ , where  $\Omega = \cup \Omega^e$  and  $\Omega^i \cap \Omega^j = \emptyset$ . Given the test functions  $S^h$  and the space of admissible variations  $V^h$ , respectively defined by:

$$S^h = \{ \mathbf{U}^h / \mathbf{U}^h \in [\mathbf{H}^{1h}(\Omega)]^5, \mathbf{U}^h / \Omega_e \in [P^1(\Omega^e)]^5, \mathbf{U}^h \cdot \mathbf{e}_k = g_k \text{ in } \Gamma_{gk} \} \quad (11)$$

$$V^h = \{ \mathbf{W}^h / \mathbf{W}^h \in [\mathbf{H}^{1h}(\Omega)]^5, \mathbf{W}^h / \Omega_e \in [P^1(\Omega^e)]^5, \mathbf{W}^h \cdot \mathbf{e}_k = 0 \text{ in } \Gamma_{gk} \} \quad (12)$$

where  $\mathbf{H}^{1h}(\Omega)$  is a finite dimensional space over  $\Omega$ ,  $P^1(\Omega^e)$  represents polynomials of first order in  $\Omega^e$  and  $\Gamma_g$  is the contour of  $\Omega$  with Dirichlet prescribed conditions. Considering a standard discretization of  $\Omega$  into finite elements, the SUPG formulation for the Euler equations in conservation variables introduced by Tezduyar and Hughes (1982, 83), supplemented by a shock-capturing operator is written as,

$$\int_{\Omega} \mathbf{W}^h \cdot \left( \frac{\partial \mathbf{U}^h}{\partial t} \mathbf{A}_i^h \frac{\partial \mathbf{U}^h}{\partial x_i} \right) d\Omega + \sum_{e=1}^{nel} \int_{\Omega^e} (\mathbf{A}_k^h)^t \boldsymbol{\tau} \left( \frac{\partial \mathbf{W}^h}{\partial x_k} \right) \cdot \left[ \frac{\partial \mathbf{U}^h}{\partial t} + \mathbf{A}_i^h \frac{\partial \mathbf{U}^h}{\partial x_i} \right] d\Omega + \sum_{e=1}^{nel} \int_{\Omega^e} \delta \left( \frac{\partial \mathbf{W}^h}{\partial x_i} \right) \frac{\partial \mathbf{U}^h}{\partial x_i} d\Omega = 0 \quad (13)$$

The stabilization matrix  $\boldsymbol{\tau}$  is defined through diagonal matrices. This form of stabilization was initially introduced by Hughes and Tezduyar (1984) and it was improved by Aliabadi *et al.* (1993). The matrix  $\boldsymbol{\tau} = \tau \mathbf{I}$  depends on the parameter  $\tau$  that is defined as:

$$\tau = \max[0, \tau_l + \zeta(\tau_a - \tau_\delta)] \quad (14)$$

$$\tau_l = \frac{2}{3(1 + 2\alpha CFL)} \tau_a \quad (15)$$

$$\tau_a = \frac{h}{2(c + |\mathbf{u}\boldsymbol{\beta}|)} \quad (16)$$

$$\tau_\delta = \frac{\delta}{(c + |\mathbf{u}\boldsymbol{\beta}|)^2} \quad (17)$$

where  $\tau_t$  is the stabilization parameter correspondent to time-dependent terms,  $\tau_a$  is the stabilization parameter correspondent to the advective terms,  $\tau_\delta$  is the stabilization parameter to discount the effects of shock-capturing operator,  $c$  is the acoustic speed and  $h$  is the mesh parameter defined as  $V^{1/3}$ , where  $V$  is the element volume. The parameter  $\zeta$  is a coefficient utilized in the time integration algorithm and  $CFL$  is the Courant-Friedrichs-Lewy number, both defined as

$$\zeta = \frac{2\alpha CFL}{1 + 2\alpha CFL} \quad (18)$$

$$CFL = \frac{(c + |\mathbf{u}\boldsymbol{\beta}|)\Delta t}{h} \quad (19)$$

and  $\boldsymbol{\beta}$  is an arbitrary normalized vector given by:

$$\boldsymbol{\beta} = \frac{\nabla \|\mathbf{U}\|_*^2}{\|\nabla \|\mathbf{U}\|_*^2\|_2} \quad (20)$$

where  $\|\cdot\|_* = \|\cdot\|_2$  or  $\|\cdot\|_{\tilde{\mathbf{A}}_0^{-1}}$ ,  $\alpha$  is a parameter controlling the stability and accuracy of the time-marching algorithm and  $\Delta t$  is the time-step. In this work we adopt  $\alpha = 0.5$ . The shock-capturing parameter  $\delta_{CAU}$  can be defined as in Almeida and Galeão (1996) as

$$\delta_{CAU} = \frac{\left\| \frac{\partial \mathbf{U}^h}{\partial t} + \mathbf{A}_x \frac{\partial \mathbf{U}^h}{\partial x} + \mathbf{A}_y \frac{\partial \mathbf{U}^h}{\partial y} + \mathbf{A}_z \frac{\partial \mathbf{U}^h}{\partial z} \right\|_{\tilde{\mathbf{A}}_0^{-1}}}{\left\| \nabla_\xi \mathbf{U}^h \right\|_{\tilde{\mathbf{A}}_0^{-1}}} \quad (21)$$

$$\begin{aligned} \left\| \nabla_\xi \mathbf{U}^h \right\|_{\tilde{\mathbf{A}}_0^{-1}} &= \left\| \frac{\partial x}{\partial \xi_1} \frac{\partial \mathbf{U}^h}{\partial x} + \frac{\partial y}{\partial \xi_1} \frac{\partial \mathbf{U}^h}{\partial y} + \frac{\partial z}{\partial \xi_1} \frac{\partial \mathbf{U}^h}{\partial z} \right\|_{\tilde{\mathbf{A}}_0^{-1}} \\ &+ \left\| \frac{\partial x}{\partial \xi_2} \frac{\partial \mathbf{U}^h}{\partial x} + \frac{\partial y}{\partial \xi_2} \frac{\partial \mathbf{U}^h}{\partial y} + \frac{\partial z}{\partial \xi_2} \frac{\partial \mathbf{U}^h}{\partial z} \right\|_{\tilde{\mathbf{A}}_0^{-1}} + \left\| \frac{\partial x}{\partial \xi_3} \frac{\partial \mathbf{U}^h}{\partial x} + \frac{\partial y}{\partial \xi_3} \frac{\partial \mathbf{U}^h}{\partial y} + \frac{\partial z}{\partial \xi_3} \frac{\partial \mathbf{U}^h}{\partial z} \right\|_{\tilde{\mathbf{A}}_0^{-1}} \end{aligned} \quad (22)$$

if  $\left\| \nabla_\xi \mathbf{U}^h \right\|_{\tilde{\mathbf{A}}_0^{-1}} \neq 0$ , and on the contrary  $\delta_{CAU} = 0$ . The components  $\partial x_i / \partial \xi_j$  are the terms of the transformation matrix

between the physical coordinates and the local coordinates of the elements. The operator  $\delta_{CAU}$  was deduced starting from as definition in entropy variables given in Almeida and Galeão (1996), applying inverse transformations. It is employed in the variational formulation (13) an approximation by linear tetrahedral finite elements, where  $\mathbf{U}^h = \mathbf{N}(\mathbf{x})\mathbf{v}(t)$ ,  $\mathbf{N}$  are linear test functions and  $\mathbf{v}$  are functions dependent on time only. Such approximation produces a set of coupled nonlinear ordinary differential equations given by

$$\mathbf{M}\mathbf{a} + \mathbf{C}\mathbf{v} = \mathbf{0} \quad (23)$$

where  $\mathbf{v}$  is the vector of nodal values of  $\mathbf{U}$ ,  $\mathbf{a}$  is the derivative of  $\mathbf{v}$  with respect to time,  $\mathbf{M}$  is the generalized mass matrix,  $\mathbf{C}$  is the generalized convection matrix.

To solve the non-linear system (23) is used a Predictor-Multicorrector algorithm as presented in a general form in Hughes (1987) and more focused on compressible flows in Aliabadi *et al.* (1993). The resulting effective systems of linearized equations are solved by the GMRES algorithm with nodal block diagonal pre-conditioning as in Shakib (1988). All matrix coefficients and residual terms have been computed explicitly with the aid of symbolic algebra software. Thus, the routines to compute the left hand side element matrices and the right-hand side residual vector contains only single loops sweeping all elements in the mesh.

### 3.1. Matrix-vector products

Even though we adopted a quasi-linear form of the Euler equations, the problem is still strongly non-linear and presents several shocks. To drive fast and accurate an steady state solution it is important to choose a suitable manner to treat the non-linearities. In the first approach, element contributions to the jacobian matrices are computed and stored. Matrix-vector products are computed by using element-by-element (ebe) loops. The main drawback of this strategy is its extensive memory requirements. For instance, when using a PC, this could be a limiting factor for large-scale analysis.

The other approach adopted herein is the so-called Jacobian-Free Newton-Krylov (JFNK) method (Knoll and Keyes, 2004) where there is a connection between the non-linear methods and the solver itself. The Jacobian matrix is not stored, trading memory requirements for computer processing time. The matrix-vector products ( $\mathbf{J}\mathbf{x}$ ) performed within GMRES are approximated by finite differences. Thus, two residual calculations are performed and the product is then approximated by

$$\mathbf{J}(\mathbf{v})\mathbf{x} = \frac{\mathbf{R}(\mathbf{v} + \varepsilon\mathbf{x}) - \mathbf{R}(\mathbf{v})}{\varepsilon} \quad (28)$$

where  $\varepsilon$  is a very small number. Here we adopt  $\varepsilon = 10^{-6}$  because preliminary tests with  $10^{-15} \leq \varepsilon \leq 10^{-6}$  did not show much sensitivity to this parameter.

### 4. Convergence acceleration techniques

Two convergence acceleration techniques towards steady state were implemented and tested on typical examples with structured and unstructured grids. The first one is the freezing of shock capturing operator introduced within finite elements by Catabriga and Coutinho (2002). This idea follows Venkatakrishnan (1995) for finite volumes. In this approach, the operator is frozen, rather arbitrarily, after a fixed number of time steps or when a measure of convergence stagnation is observed. A simple heuristic is employed to detect stagnation and we stop updating the  $\delta$  operator from that point on. In general, the non-linear problem converges very fast towards a steady state solution, reaching very low orders of magnitude and eventually machine zero. The idea is to compare the average L2 norm of the density residual ( $\rho_{avg}$ ) computed within a predetermined number of steps (say 30 to 50, for instance) with the maximum ( $\rho_{max}$ ) and minimum ( $\rho_{min}$ ) values of the same norm at a time interval. We then check if the upper and lower limits are bounded within a narrow range around the average value, that is,

$$res_{min} \geq f_{mi} res_{avg} \text{ and } res_{max} \leq f_{max} res_{avg} \quad (29)$$

when and if such conditions are satisfied, we consider that solution has stagnated, and freeze the shock capturing operator. Here the limiters  $f_{min}$  and  $f_{max}$  are taken to be 1.2 and 0.8 respectively.

The second scheme is a local time-stepping strategy. It evaluates different time steps for each element, according to a pre-defined CFL condition. Recall eq. (19) for the definition of the CFL number. It is interesting to observe that the CFL condition may be increasing when evolving to steady state, see Catabriga and Coutinho (2002) for two dimensional finite element applications.

### 5. Numerical experiments

In this section we show the solution of some classical inviscid flow problems. The first one is the one-dimensional steady shock to validate the three dimensional code. We present then two two-dimensional problems, an oblique shock and a reflected shock. All examples presented in Shakib (1988) and have closed solutions. For all cases were adopted a CFL = 1 condition to compute the analysis timestep, except for the unstructured mesh of the reflected shock example that used a CFL = 10. All solutions were obtained in a PC, with 2.0 Gbytes of memory and 2.4 GHz of processing power and run with the three dimensional code.

#### 5.1. One-dimensional steady shock

This problem models a one-dimensional steady flow of a inviscid fluid at Mach 2.0 with a normal shock. Supersonic flow enters the normal shock and subsonic flow exits the shock. The computational domain is defined by the interval  $0 \leq x \leq 39$ ,  $-0.5 \leq y \leq 0.5$  and  $-0.5 \leq z \leq 0.5$ . The finite element mesh with 936 elements and 360 nodes is shown in Fig. (1).

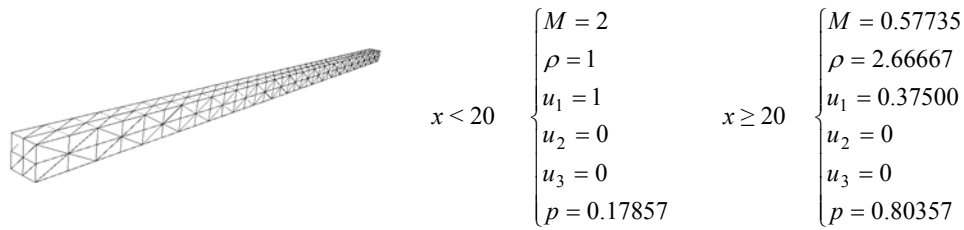


Figure 1. Mesh for the steady shock problem and initial conditions.

Densities, velocities and total specific energy are prescribed at the inflow and only total specific energy at the exit. Velocity components  $u_2$  and  $u_3$  are prescribed null at all times. At the Fig. (2) we have the density profile solution that is in agreement with the exact solution. It is also important to notice that the solution without the shock capturing term (SUPG only) is good but does not represent the shock adequately as the others do.

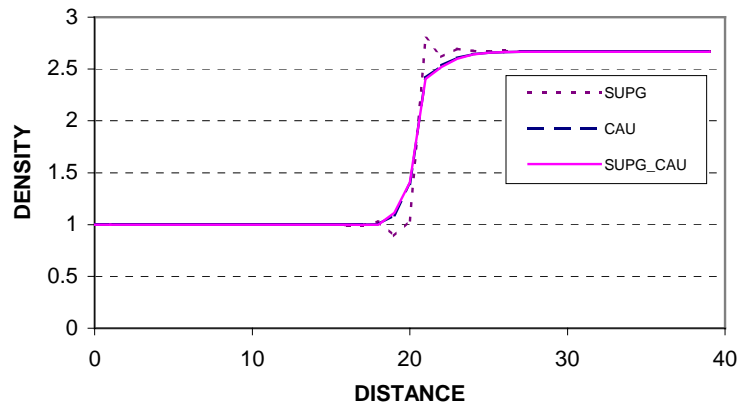


Figure 2. Density profile for the steady shock problem.

### 5.2. Two-dimensional oblique shock

This problem consists in a supersonic two-dimensional flow (Mach number  $M=2$ ) of an inviscid fluid across a slip surface. The flow meets the surface at a 10 degree angle, see Fig. (3) for further details and problem description. An oblique shock wave reflects at a 29.3 degree angle. The computational domain is defined by the interval a unit squares and a small thickness at the  $z$  direction. Two meshes were considered. A structured one with 882 nodes and 2000 elements and a non-structured with 750 nodes and 2859 elements. All elements concerned are linear tetrahedral and the front view of both meshes can be appreciated in Fig (4) along with density contours results. GMRES tolerance was set to  $10^{-3}$  with 50 krylov vectors and a limit of 15 non-linear iterations. Boundary conditions at inflow and outflow (BC) and exact solution below the shock region are given in Fig. (3). Initial conditions are taken as free-stream values. The no flow boundary condition of  $u_2 = 0$  is imposed at the bottom of the domain and the supersonic outflow has no prescription at all.

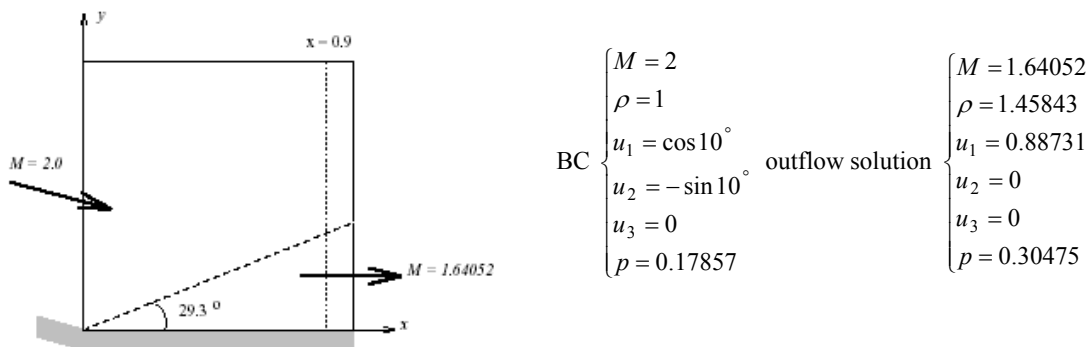


Figure 3. Oblique shock problem description.

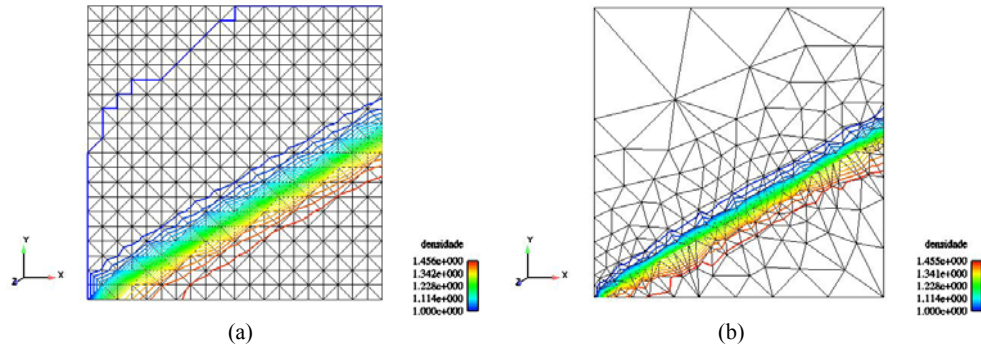


Figure 4. Solutions in terms of density contours for the oblique shock: structured (a) and unstructured (b).

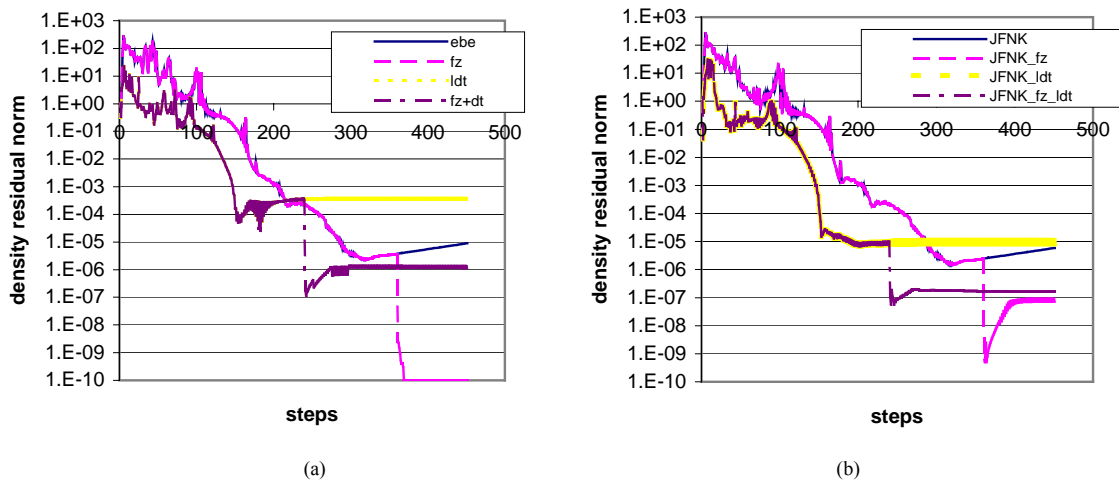


Figure 5. Evolution of density residual for the structured case: ebe (a), JFNK (b).

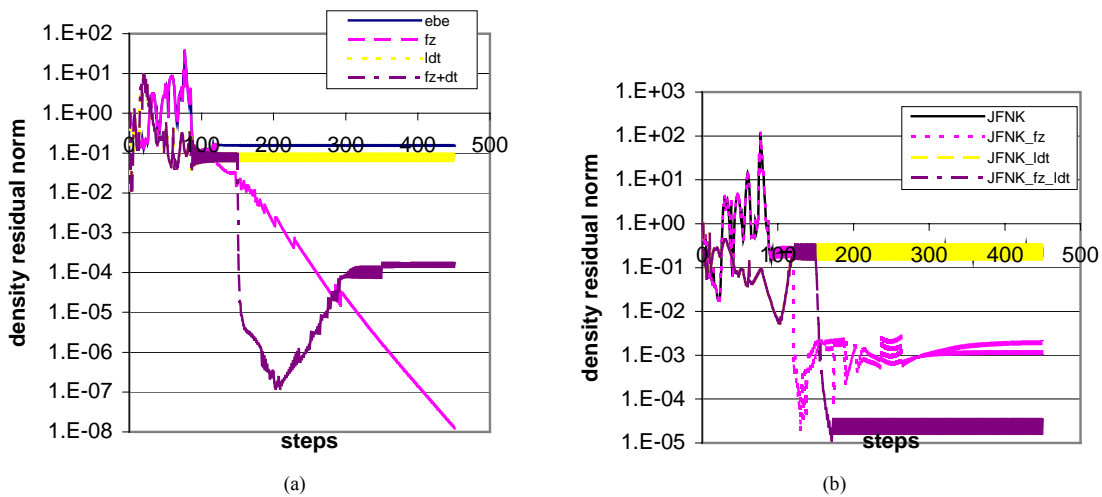


Figure 6. Evolution of density residual for the unstructured case: ebe (a), JFNK (b).

By the results presented in terms of the density residual norm in figures (5) and (6) it is possible to observe the residual stagnation, even though a stationary condition has been achieved. The freezing of the shock capturing operator (fz), as well as the local time-stepping (ldt) techniques did improve the convergence by dropping the residual a few orders of magnitude. It was also observed that both techniques worked better with the unstructured mesh, what is

considered a good aspect as long as we are interested in complex three-dimensional geometries and adaptive mesh refinement methods.

By analyzing Table 1, it can be verified that the JFNK method can be rather expensive. In order of 3 to 5 times more time consuming than the elementwise exact Jacobian. On the other hand, memory costs for the JFNK method on the structured mesh were in the order of 0.36 of the ebe method and 0.26 for the unstructured case, what makes some large-scale analysis feasible in a PC, for instance. It is also interesting to notice that for the structured mesh the acceleration strategies had almost the same processing time, while for the unstructured case the freezing technique was rather faster and the local time-stepping was a bit more expensive, compared to the usual manner. We believe that is an important observation because we are interested in fast and accurate solutions, that is, adopt one convergence technique, or a set of them, which improves convergence but does not affect computer processing times.

Table 1 – Relative processing time for the oblique shock example.

Run type	Structured mesh	Unstructured mesh
control	1.000	1.000
fz	1.007	0.315
ldt	1.005	1.791
fz + ldt	0.945	0.970
JFNK	3.782	5.187
JFNK fz	3.578	3.906
JFNK ldt	5.344	8.774
JFNK fz + ldt	5.102	8.050

### 5.3. Two-dimensional reflected shock

The problem consists of a rectangular domain ( $0 \leq x \leq 4.1$  and  $0 \leq y \leq 1.0$ ) with three regions of flows partitioned by shocks, as shown in Fig. (7). The prescribed boundary conditions are density, velocities and total specific energy at the left and top boundaries. At the bottom boundary, a no flow boundary condition is imposed, *i.e.*  $u_2 = 0$ . At the right boundary there is no prescription, since the outflow is supersonic. GMRES tolerance was set to  $10^{-1}$  with a limit of 5 non-linear iterations. A view of the structured mesh with 3402 nodes and 8000 elements and of the unstructured mesh with 27944 nodes and 142075 elements is shown in Fig. (8) along with density contours solutions.

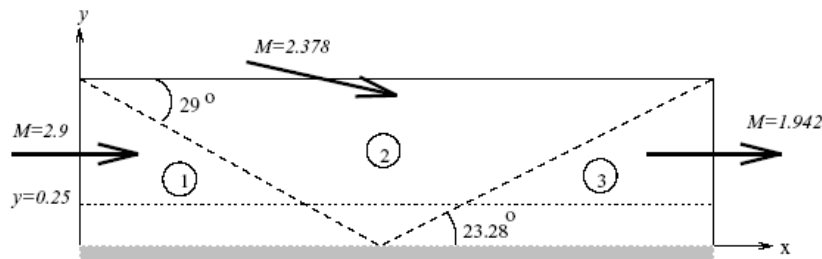
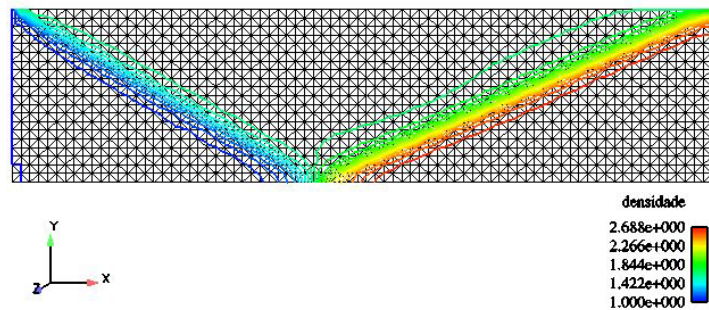


Figure 7. Reflected shock problem description.



(a)

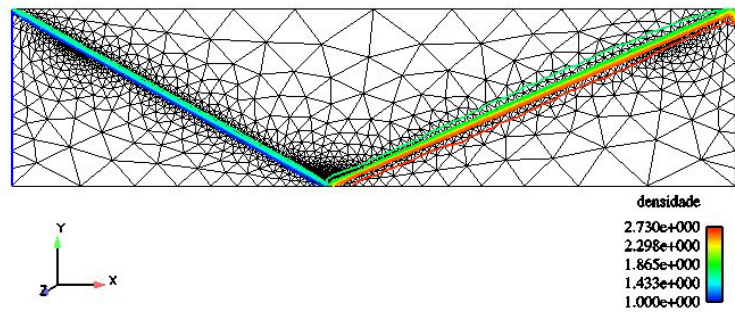


Figure 8. Solutions in terms of density contours for the reflected shock: structured (a) and unstructured (b).

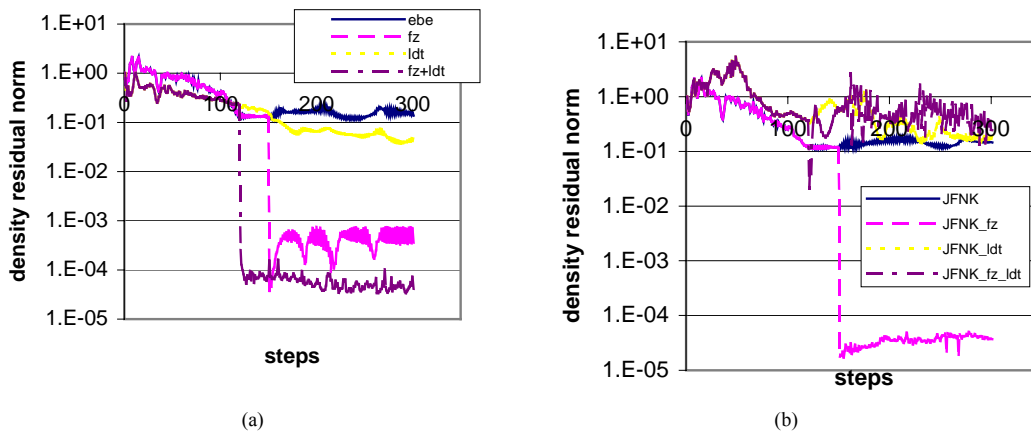


Figure 9. Evolution of density residual for the structured case: ebe (a), JFNK (b).

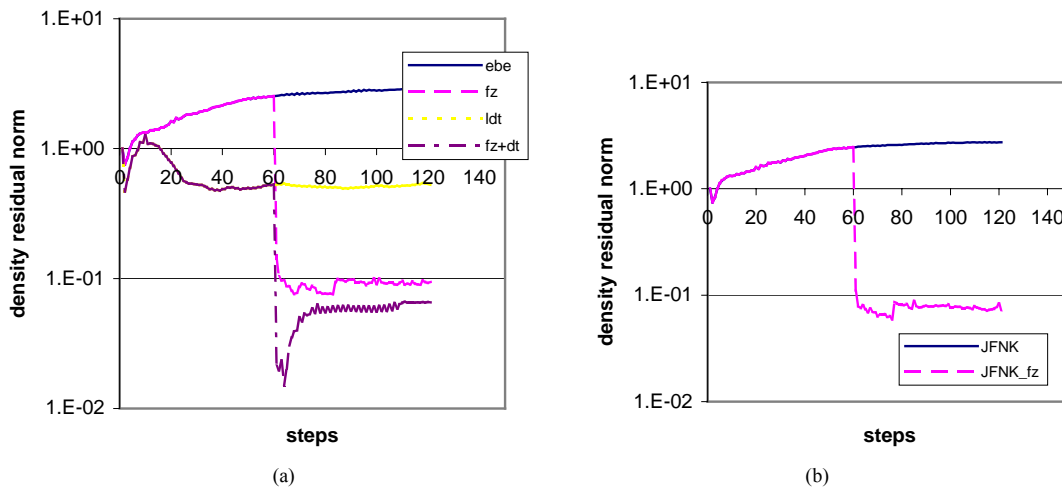


Figure 10. Evolution of density residual for the unstructured case (CFL = 10): ebe (a), JFNK(b).

In this example the results seemed more promising, according to figures (9) and (10). Note that, for the structured case, the JFNK approach did not increase non-linear convergence as desired. On the other hand, the freezing technique did improve drastically in this example. It is to mention that the results for the local time-stepping strategy did improve convergence only a bit and for the unstructured case results were not available, because convergence failed. As before the freezing technique did improve convergence very fast as soon as the shock capturing operator stopped being updated. Again processing time for the JFNK approach is higher than for the ebe, as can be seen in Table 2. Although, memory costs for the JFNK method were 0.35 of the ebe demanded memory for the structured case and 0.22 for the unstructured case.

Table 2 – Relative processing time for the reflected shock example.

Run type	Structured mesh	Unstructured mesh
control	1.000	1.000
fz	0.981	1.301
ldt	0.718	0.617
fz + ldt	0.324	1.078
JFNK	1.254	2.401
JFNK fz	2.396	8.916
JFNK ldt	2.319	-
JFNK fz + ldt	1.785	-

## 6. Conclusions

We presented numerical tests with the objective to gain some convergence acceleration towards steady state solutions for the compressible Euler equations. Two approaches account for treating the Jacobian matrix. In the first the Jacobian matrix is stored and matrix-vector products within the GMRES iterative solver are performed elementwise in a direct manner. In the Jacobian free case, the matrix-vector product is approximated by finite differences, saving memory requirements but spending more processing time. Although the latter strategy helps nonlinear convergence it is more time consuming, in the order up to 5 times more. In our case the JFNK method did not improve non-linear convergence as desired, possibly due to the quasi-linear form of the Euler equations adopted here.

In the experiments driven for two dimensional problems the freezing was the most effective technique. The local time stepping also reduced residual norms, but in a minor sense. The convergence acceleration techniques were very effective on the simple test cases of this study. Further tests on typical three-dimensional problems, such as flows around aerospace vehicles, which are geometrically complex, are of main interest.

## 7. Acknowledgement

The authors would like to thank the helpful discussions with Dr. L. Catabriga from the Federal University of Espirito Santo (UFES), Brazil.

## 8. References

- Aliabadi S. K., Ray S. E., Tezduyar T. E., 1993, "SUPG finite element computation of viscous compressible flows based on the conservation and entropy variables formulations", *Computational Mechanics*, vol. 11, pp. 300-312.
- Almeida R. C., Galeão A. C., 1996, "An adaptative Petrov-Galerkin formulation for the compressible Euler and Navier-Stokes equations", *Comp Appl. Mech. and Engng.*, vol. 129, pp. 157-176.
- Catabriga L., Coutinho A.L.G.A., 2002, "Improving convergence to steady state of implicit SUPG solution of Euler equations", *Commun. Numer. Meth. Engng.*, vol. 18, pp. 345-353.
- Hirsch C., 1992, *Numerical computation of internal and external flows, volume 2 – Computational Methods for Inviscid and Viscous Flows*, John Wiley and Sons Ltd, Chichester.
- Hughes, T. J. R., *The Finite Element Method – Linear Static and Dynamic Finite Element Analysis*, Englewood Cliffs, NJ, Prentice-Hall, 1987.
- Hughes T. J. R., Franca L. P., Mallet M., 1986, "A new finite element formulation for computational fluid dynamics: I. Symmetric forms of the compressible Euler and Navier-Stokes equations and the second law of thermodynamics", *Comp. Meth. Appl. Mech. and Engng.*, vol. 54, pp. 223-234.
- Hughes T. J. R., Tezduyar T. E., 1984, "Finite element methods for first-order hyperbolic systems with particular emphasis on the compressible Euler equations", *Comp. Meth. Appl. Mech. and Engng.*, vol. 45, pp. 217-284.
- Johan Z., Hughes T.J.R., Shakib F., 1991, "A globally convergent matrix-free algorithm for implicit time-marching schemes arising in finite element analysis in fluids", *Comp. Meth. Appl. Mech. and Engng.*, vol. 87, pp. 281-304.
- Johnson C., Szepessy A., Hansbo P. 1990, "On the convergence of shock-capturing streamline diffusion finite element methods for hyperbolic conservation laws", *Mathematics of Computation* 54, 107-129.
- Knoll D.A., Keyes D.E., 2004, "Jacobian-free Newton–Krylov methods: a survey of approaches and applications", *Journal of Computational Physics*, vol. 193, pp. 357-397.
- Shakib F., 1988, "Finite element analysis of the compressible Euler and Navier-Stokes equations", Ph.D. thesis, Department of Mechanical Engineering, Stanford University.
- Tezduyar, T. E., Hughes, T. J. R., 1982, "Development of time-accurate finite element techniques for first-order hyperbolic systems with particular emphasis on the compressible Euler equations", NASA Technical Report NASA-CR-204772, NASA.

- Tezduyar, T. E., Hughes, T. J. R., 1983, "Finite element formulations for convection dominated flows with particular emphasis on the compressible Euler equations", 21 st Aerospace Sciences Meeting, Reno, Nevada, AIAA, vol. 83-0125.
- Venkatakishnan, V., 1995, "Convergence to Steady State Solutions of the Euler Equations on Unstructured Grids with limiters", Journal of Computational Physics, vol. 118, pp. 120-130.